analytical chemistry

pubs.acs.org/ac

Article

Dual-Locked Near-Infrared Fluorescent Probes for Precise Detection of Melanoma via Hydrogen Peroxide−Tyrosinase Cascade Activation

Haiyue Peng, Ting Wang, Guorui Li,* Jing Huang,* and Quan Yuan

Cite This: https://doi.org/10.1021/acs.analchem.1c04058

Read Online

ACCESS | Metrics & More | Article Recommendations | Supporting Information

ABSTRACT: Activity-based near-infrared (NIR) fluorescent probes provide powerful tools for diagnosis of diseases. However, most of these probes suffer from low specificity due to "off-target" reaction. The dual-locked strategy, which utilizes two biomarkers as triggers, can increase the specificity and precision of diagnosis. Here, we report a dual-locked NIR probe, **MB-*m*-borate**, which releases fluorophore methylene blue (**MB**) after hydrogen peroxide−tyrosinase (H_2O_2-TYR) cascade activation. Both **MB-*m*-borate** and its intermediate **MB-*m*-phenol** (the product after H_2O_2 activation) show almost non-detectable fluorescence. **MB-*m*-borate** exhibits "turn on" fluorescence upon H_2O_2-TYR cascade activation. The further live cell bioimaging results indicate that **MB-*m*-borate** only responds to melanoma cells, providing it as a robust probe for precise detection of melanoma. Finally, the probe is applied for the diagnosis of melanoma in vivo with a xenogeneic mouse model.

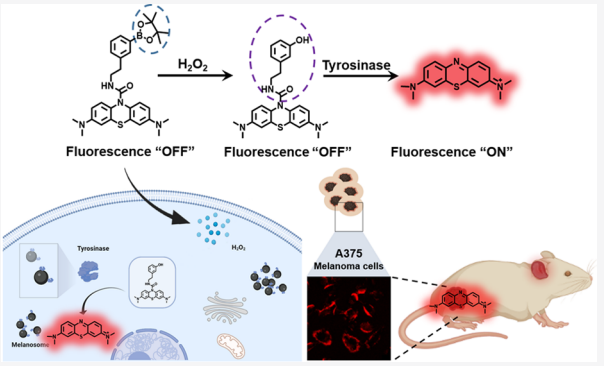

INTRODUCTION

Cancer is a big threat to human health.[1] The precise diagnosis of cancer is especially important because it is a prerequisite for cancer treatment. A convenient method that can be used for cancer screening with minimal interference to patients is highly demanded. Biomarker-activated fluorescent probes, especially near-infrared (NIR) fluorescent probes provide powerful methods for diagnosis of diseases.[2−5] This strategy exploits endogenous biospecies in tumors to activate probes and turn on fluorescence.[6] Nevertheless, many fluorescent probes suffer from low specificity, which is caused by the "off-target" effect, resulting in false-positive results or high background signals. It is difficult to precisely differentiate cancer phenotypes by one single biomarker. To circumvent the low specificity, dual or multiple biomarker-activated probes attract much attention in recent years.[7−13]

Melanoma is one of the most malignant skin diseases, which can easily migrate. Statistics show that the five-year relative survival rate for the early stage of skin melanoma is 98%; however, it drops to 23% when melanoma progresses to the late stage.[14] Thus, precise diagnosis of melanoma at the early stage is vital. Among the biomarkers for melanoma, tyrosinase (TYR) is of interest because it naturally catalyzes the biosynthesis of melanin.[15,16] High levels of TYR are expressed in melanoma cells, making it as an ideal target for melanoma diagnosis or treatment. TYR can convert phenol to catechol and then to quinone.[15,17] Based on this reaction, various TYR-activated probes or prodrugs have been developed.[18−24] As shown in Figure 1A, recently, the Ma group[22] reported a TYR-activated NIR probe, which utilized 3-hydroxybenzyloxy as a recognition moiety to increase its specificity toward TYR and minimize the interference from other oxidants. However, these TYR-activated probes might not precisely detect melanoma because TYR is also involved in normal melanocytes formation.[16] A dual-biomarker-triggered probe may address this issue. Many cancers, including melanoma, are associated with the high level of reactive oxygen species (ROS). As a main component of ROS, hydrogen peroxide (H_2O_2) has 10 times the content in cancer cells than that in normal cells.[25] Figure 1B showed the first H_2O_2 fluorescent probe developed by Chang and coworkers,[26] which exploited boron chemistry and released the fluorophore after H_2O_2 activation. After that, multiple H_2O_2 fluorescent probes have been discovered.[27−35] Inspired by these studies, we envision that a high level of H_2O_2 and TYR in melanoma may be explored for the development of a dual-locked NIR fluorescent probe in the precise detection of melanoma.

To this end, we report a NIR fluorescent probe methylene blue (**MB**)-***m*-borate.** This probe remains locked until it is

Received: September 17, 2021
Accepted: December 16, 2021

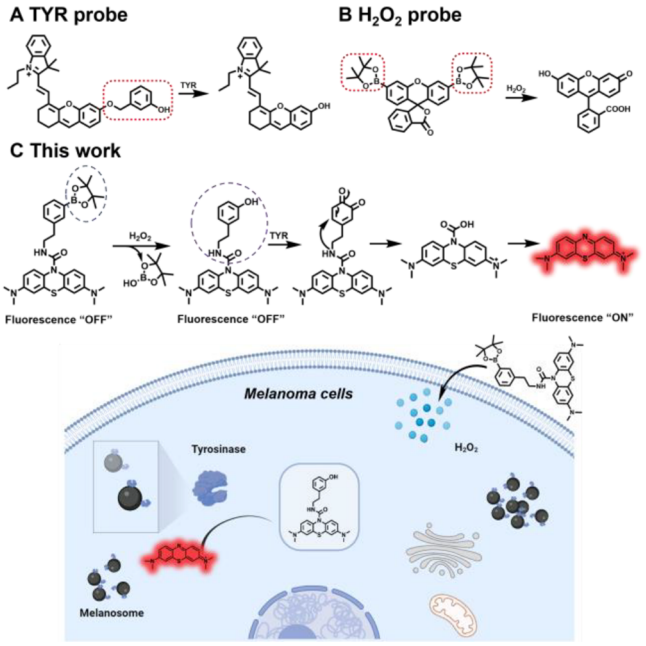

Figure 1. (A) TYR probe using *m*-phenol as the recognition moiety; (B) classical hydrogen peroxide probe; (C) ***this work***: H_2O_2-TYR cascade-activated probe for the precise detection of melanoma.

cascade-activated by H_2O_2 and TYR, resulting in a strong fluorescence "turn on" signal in melanoma (Figure 1C).

EXPERIMENTAL SECTION

Synthesis. The probe **MB-*m*-borate** was synthesized and characterized by ^{1}H NMR, ^{13}C NMR, and high-resolution mass spectrometry (HRMS). The detailed synthesis and characterization of all these compounds are given in the Supporting Information.

High-Performance Liquid Chromatography Assay. The gradient consisted of five parts: 0−4 min, 95% A−5% B; 4−15 min, from 95% A−5% B to 5% A−95% B; 15−20 min, 5% A−95% B; 20−25 min, from 5% A−95% B to 95% A−5% B; 25−26 min, 95% A−5% B. Phase A: H_2O containing 0.03% trifluoroacetic acid (TFA); Phase B: acetonitrile. Other high-performance liquid chromatography (HPLC) conditions were as follows: temperature of 30 °C; flow rate of 1 mL/min; and monitoring wavelength of 260 nm.

Live Cell Imaging. Cells were seeded on 3.5 cm confocal dish. **MB-*m*-borate** or **MB-*m*-phenol** (20 μM) was added and incubated for 2 h. After three times washing, cells were imaged on a fluorescence confocal microscope (Nikon A1 R MP, λ_{ex} 647 nm; λ_{em} 663−738 nm). In experiments with inhibitors, A375 cells were pretreated with 200 μM kojic acid or *N*-acetyl-L-cysteine (NAC) for 2 h. Then, the cells were cultured with 20 μM **MB-*m*-borate** or **MB-*m*-phenol** in the presence of 200 μM kojic acid or NAC for another 2 h.

Establishment of the Mouse Model and In Vivo Bioimaging with MB-*m*-borate. The BALB/c-nu female mice were subcutaneously injected with 1×10^7 A375 cells to form melanoma entity. After 2 weeks, 12 BALB/c-nu female mice bearing melanoma were randomly assigned into four groups (A/B/C/D). The mice in group A were intratumorally injected with a vehicle (5% dimethylsulfoxide, DMSO; 2% Tween 80, 10% PEG-300, 83% saline). For group B, the mice were intratumorally injected with **MB-*m*-borate** (2 mM, 100 μL). The mice in group C were pretreated with NAC (5 mM, 100 μL) for 1 h, and then injected with 100 μL of mixture containing **MB-*m*-borate** (2 mM) and NAC (5 mM). The mice in group D were pretreated with kojic acid (10 mM, 100 μL) for 1 h and then injected with 100 μL of mixture containing **MB-*m*-borate** (2 mM) and kojic acid (10 mM). After 1 h, these mice were anesthetized prior to imaging. The images were collected using Caliper VIS Lumina XR. All animal procedures were approved by the Administrative Committee on Animal Research at Hunan University, under the license Hnubio202102001.

RESULTS AND DISCUSSION

Design and Synthesis of the Probe MB-*m*-borate. To construct an activity-based probe, two moieties are needed: the signal group and the recognition moiety. For the signal moiety, **MB** was selected in view of two factors: one is it can be easily modified so that a recognition moiety can be conveniently attached,[24] and the other is **MB** emits NIR fluorescence with a wavelength of 684 nm, which is suitable for bioimaging.[36] For the recognition moiety, we choose the borate group as the first trigger because of its good response to H_2O_2. The 3-hydroxybenzyloxy group is used as the second trigger because it served as the TYR substrate with high specificity.[22] Taken together, the probe **MB-*m*-borate** was designed, which had **MB** as the signal moiety, and *m*-phenyl-borate as the recognition moiety (Figure 1C). We speculated **MB-*m*-borate** can be activated by H_2O_2 to produce **MB-*m*-phenol**, and then, further TYR activation would remove the entire phenol group to produce the fluorophore **MB** (Figure 1C).

The probe **MB-*m*-borate** can be easily synthesized by four steps using **MB** as the starting material (Scheme 1). First, **MB**

Scheme 1. Synthesis of MB-*m*-borate. (1) $Na_2S_2O_4$, $NaHCO_3$, DCM, H_2O, RT; (2) TPG, TEA; (3) TEA, 3-Bromophenethylamine; (4) KOAc, Pd(dppf)Cl_2, Bis(pinacolato) diboron; (5) H_2O_2, MeOH

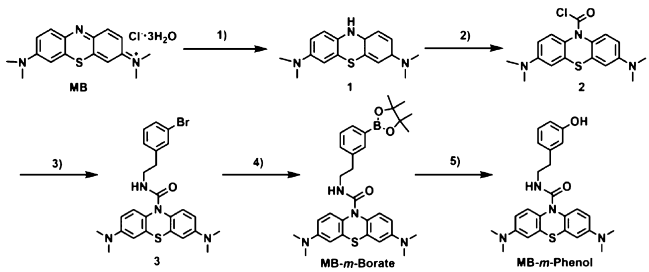

was reduced using sodium hydrosulfite to produce compound **1**, which was treated with triphosgene to afford compound **2**. Then, it was coupled with 3-bromophenethylamine to obtain compound **3**. Finally, the probe **MB-*m*-borate** was obtained by Miyaura borylation reaction using bis(pinacolato)diboron. The intermediate **MB-*m*-phenol** was synthesized by the treatment of **MB-*m*-borate** with excess H_2O_2. The detailed synthesis and characterization of these compounds are given in the Supporting Information.

Chemical Transformation of MB-*m*-borate by H_2O_2 and TYR. With **MB-*m*-borate** in hand, we tested its chemical transformation by HPLC analysis. As shown in Figure 2A, the retention time (RT) of **MB-*m*-borate** is 17.7 min. In addition to this peak, another peak with RT 13.2 min was identified to be its hydrolysis product **MB-*m*-boric acid** (Figure 2B). **MB-**

https://doi.org/10.1021/acs.analchem.1c04058
Anal. Chem. XXXX, XXX, XXX−XXX

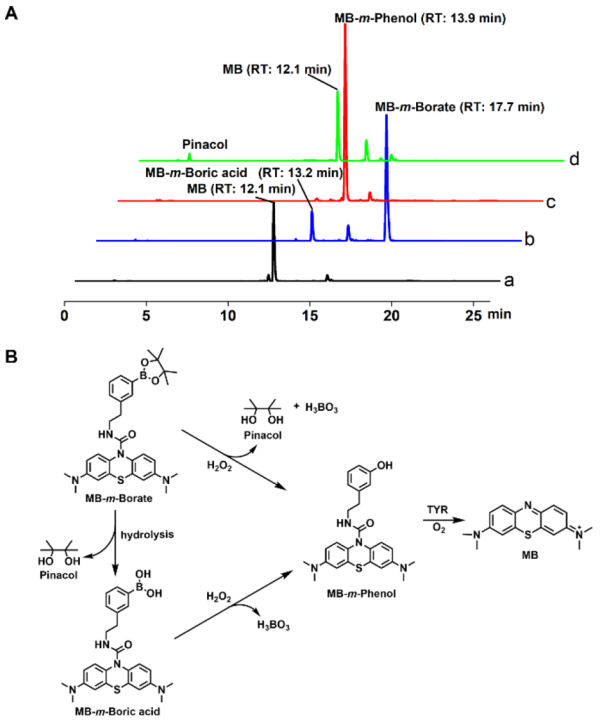

Figure 2. Conversion of **MB-*m*-borate** to **MB**. (A) HPLC analysis of **MB-*m*-borate** to **MB** (a. **MB** 50 μM; b. **MB-*m*-borate** 50 μM; c. **MB-*m*-borate** 50 μM + 10 equiv H_2O_2 1 h at 37 °C; d. **MB-*m*-phenol** 50 μM + 500 U/mL TYR 1 h at 37 °C). (B) Proposed reaction mechanism of the conversion of **MB-*m*-borate** to **MB**.

***m*-borate** can be efficiently converted into **MB-*m*-phenol** (RT 13.9 min) using H_2O_2 (10 equiv) in 1 h. It is noteworthy that **MB-*m*-borate** can be selectively activated by H_2O_2 because other oxidants, including TYR, had a negligible effect on it (Figure S1). **MB-*m*-boric acid** and **MB-*m*-phenol** were also synthesized here (see the Supporting Information). The conversion of **MB-*m*-phenol** to **MB** was also tested. **MB-*m*-phenol** was converted to **MB** (RT 12.1 min) by TYR at 37 °C in 1 h. This conversion also showed good selectivity toward TYR (Figure S2). Our results also showed that these conversions are H_2O_2/TYR concentration- and time-dependent (Figures S3−S6).

Optical Behaviors of MB-*m*-borate toward H_2O_2-TYR Activation. We then examined whether conversion was accompanied with optical changes. **MB** had a UV absorption peak at 665 nm, and it exhibited strong fluorescence at 684 nm (Figures S7 and 3A). As a comparison, the fluorescence of **MB-*m*-borate** and **MB-*m*-phenol** was faint (Figure S8). This implied that **MB-*m*-borate** can be used as a "turn on" probe for H_2O_2-TYR detection. As shown in Figure 3A, **MB-*m*-borate** led to a slight fluorescence increase at 684 nm by H_2O_2 (10 equiv), which can be ascribed to the weak fluorescence of **MB-*m*-phenol**. Strikingly, the incubation of **MB-*m*-phenol** with TYR exhibited a dramatic fluorescence enhancement (~17 fold, Figure 3B). The fluorescence increase by TYR was in a concentration- and time-dependent manner (Figures S9 and S10). The fluorescence response of **MB-*m*-borate** toward H_2O_2-TYR cascade activation was further investigated. As shown in Figure 3, **MB-*m*-borate** was incubated with H_2O_2 (10 equiv) and TYR in phosphate buffered saline (PBS), a strong fluorescence was observed, and approximately a 38-fold

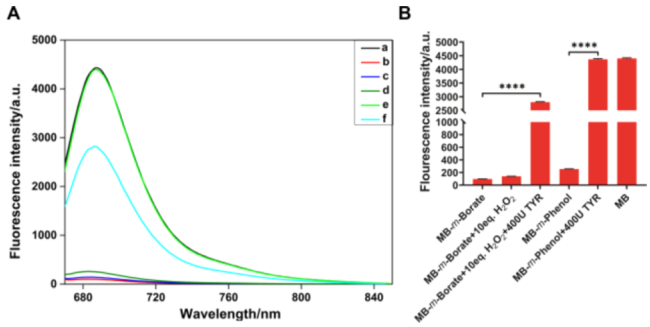

Figure 3. (A) Optical properties of the probe and its fluorescence change by H_2O_2-TYR activation (λ_{ex} 665 nm; λ_{em} 684 nm). (a. **MB** 10 μM; b. **MB-*m*-borate** 10 μM; c. **MB-*m*-borate** 10 μM + 10 equiv H_2O_2 1 h; d. **MB-*m*-phenol** 10 μM; e. **MB-*m*-phenol** 10 μM + 400 U/mL TYR 1 h.; f. **MB-*m*-borate** 10 μM +10 equiv H_2O_2 1 h + 400 U/mL TYR 1 h.) (B) Fluorescence intensity analysis from (A). ****$P < 0.0001$.

enhancement was achieved compared with the fluorescence of **MB-*m*-borate**.

MB-*m*-borate for Melanoma Bioimaging. All the above results proved our hypothesis that **MB-*m*-borate** can be cascade-activated by H_2O_2-TYR, and the fluorescence was "turned on." This prompted us to apply this probe in melanoma bioimaging. The cytotoxicity of **MB-*m*-borate** in different cell lines was tested. The results indicated that the probe show low cytotoxicity (Figure S11). The A375 cell line (human melanoma cell line), which expresses a high level of H_2O_2 and TYR,[37,38] was used as a cell model to test our hypothesis. As we expected, confocal fluorescence imaging results showed that **MB-*m*-borate** exhibited strong red fluorescence in A375 cells (Figure 4A). As a comparison,

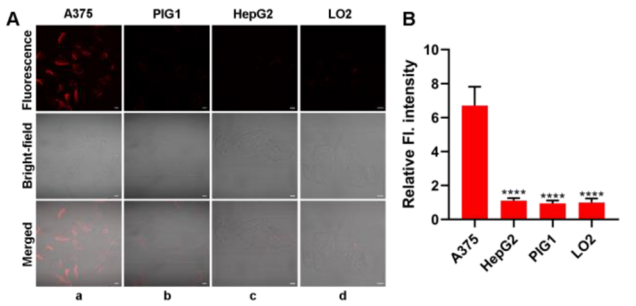

Figure 4. (A) Bioimaging of **MB-*m*-borate** (20 μM) in living cells. Scale bar, 10 μm. (B) Relative fluorescence intensity of each cell lines from (A). Six fields of cells were analyzed.

MB-*m*-borate showed negligible fluorescence in other cell lines, including PIG1 cells (human normal melanocytes cell line), HepG2 cells, LO2 cells, A549 cells, HT29 cells, M059J cells, HeLa cells, and MDA-MB-231 cells (Figures 4 and S12). The fluorescence intensity of **MB-*m*-borate** in A375 was 6.7-fold than that of LO2 cells. (Figure 4B). It is reasonable because other cell lines do not express high levels of H_2O_2 and TYR simultaneously; thus, they fail to release the fluorophore **MB**. It is worth noting that the probe can differentiate melanoma cells (A375) from normal melanocytes (PIG1). The fluorescence intensity of **MB-*m*-borate** in A375 was 7.1-fold than that of PIG1 cells. This is unachievable for other TYR-activated probes.

https://doi.org/10.1021/acs.analchem.1c04058
Anal. Chem. XXXX, XXX, XXX−XXX

To further verify the fluorescence of **MB-*m*-borate** in A375 cells is due to the activation of both H_2O_2 and TYR, we pretreated A375 cells with either a tyrosinase inhibitor, kojic acid, or an antioxidant **NAC**. A375 cells were pretreated with 200 μM kojic acid for 2 h, and then, 20 μM **MB-*m*-borate** was added and incubated for a further 2 h (Figure 5). As expected,

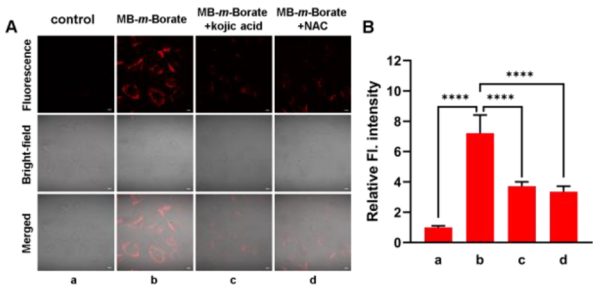

Figure 5. (A) Bioimaging of **MB-*m*-borate** in A375 cells. Scale bar, 10 μm. (a) Control (untreated). (b) A375 cells treated with 20 μM **MB-*m*-borate** for 2 h. (c) A375 cells treated with 200 μM kojic acid for 2 h and then coincubated with 20 μM **MB-*m*-borate** for another 2 h. (d) A375 cells were pretreated with 200 μM *N*-acetyl-L-cysteine (**NAC**) for 2 h, and then coincubated with 20 μM **MB-*m*-borate** for another 2 h. (B) Relative fluorescence intensity analysis from (A). Six fields of cells were analyzed. ****$P < 0.0001$.

the fluorescence intensity decreased significantly compared with the noninhibitor treated group (1.9-fold decrease, Figure 5B). A similar phenomenon was observed in **NAC**-treated A375 cells, and the fluorescence intensity reduced 2.1-fold. These results clearly demonstrate the requirement of H_2O_2-tyrosinase cascade activation for the fluorescence of **MB-*m*-borate** in A375 cells.

MB-*m*-phenol, which is the first activation product of **MB-*m*-borate** by H_2O_2, was also used for bioimaging study here. Consistent with our assumption, remarkable fluorescence of **MB-*m*-phenol** was observed in both A375 and PIG1 cells, implying the limitation of **MB-*m*-phenol** for differentiating melanoma cells from normal melanocytes (Figure S13). The effects of kojic acid and **NAC** on the fluorescence of **MB-*m*-phenol** in A375 cells were also investigated. The pretreatment of kojic acid can dramatically decrease the fluorescence. However, the effect of **NAC** was not significant (Figure 6). This result further proved that **MB-*m*-phenol** can be used for

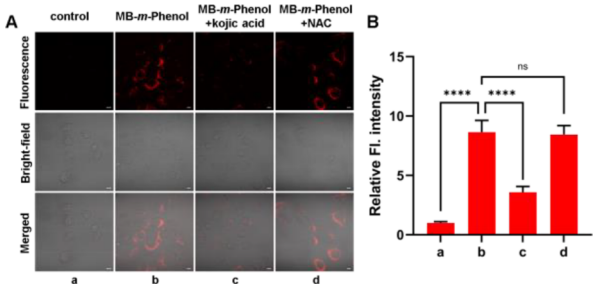

Figure 6. (A) Bioimaging of **MB-*m*-phenol** in A375 cells. Scale bar, 10 μm. (a) Control (untreated). (b) A375 cells treated with 20 μM **MB-*m*-phenol** for 2 h. (c) A375 cells treated with 200 μM kojic acid for 2 h and then coincubated with 20 μM **MB-*m*-phenol** for another 2 h. (d) A375 cells were pretreated with 200 μM N-acetyl-L-cysteine (**NAC**) for 2 h, and then coincubated with 20 μM **MB-*m*-phenol** for another 2 h. (B) Relative fluorescence intensity analysis from (A). Six fields of cells were analyzed. ****$P < 0.0001$.

TYR activity detection, but it is not good for precise detection of melanoma. A reported tyrosinase probe MB1 was also used here for bioimaging study as a comparison.[24] We found that MB1 showed remarkable fluorescence in both normal melanocytes PIG1 and melanoma cells A375 (Figure S14).

We finally evaluated the biological application of **MB-*m*-borate** in vivo. To verify its ability to detect melanoma in mice, a mouse model was established by subcutaneous injection of melanoma cells (A375) into BALB/c nude mice. The mice were kept for about 2 weeks and then divided into 4 groups, including vehicle, **MB-*m*-borate**, kojic acid/**MB-*m*-borate,** and **NAC**/**MB-*m*-borate**-treated group. As shown in Figure 7,

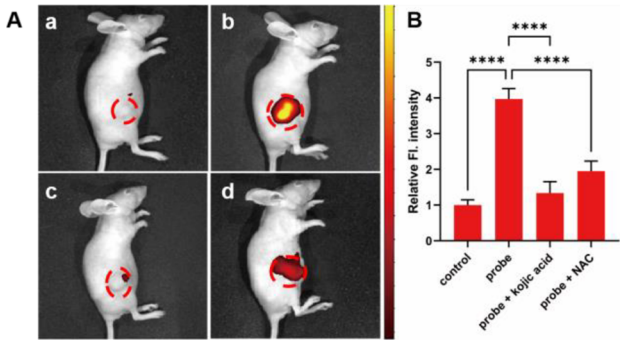

Figure 7. (A) Fluorescent images of tumor-bearing nude mice. (a) Control; (b) 2 mM **MB-*m*-borate**-treated mouse; (c) **NAC** (5 mM) and **MB-*m*-borate** (2 mM)-treated mouse; d. kojic acid (10 mM) and **MB-*m*-borate** (2 mM) treated mouse. Color scale: 9.70×10^6–2.42×10^7. (B) Quantification of the relative fluorescence intensities from A.

strong fluorescence at the tumor site was observed after 1 h of probe injection. In a sharp comparison with the control, an enhancement in the responsive fluorescence of over three fold was achieved, verifying that **MB-*m*-borate** was a promising indicator for melanoma diagnosis (Figures 7 and S15). A dramatical drop in the fluorescent intensity of **MB-*m*-borate** was observed in the mice pretreated with **NAC** or kojic acid. These data indicated that **MB** could hardly be released from **MB-*m*-borate** because of the lack of ROS or TYR in the presence of **NAC** or kojic acid.

CONCLUSIONS

In summary, a dual-locked NIR fluorescent probe **MB-*m*-borate** was developed by exploiting the endogenous high level of H_2O_2 and TYR in melanoma cells (A375 cells). The nonfluorescent **MB-*m*-borate** was converted to fluorophore **MB** by H_2O_2-TYR cascade activation, resulting in a significant fluorescence "off–on" response. **MB-*m*-borate** exhibited excellent selectivity and biocompatibility. It showed remarkable fluorescence in melanoma cells (A375 cells), but nondetectable fluorescence in other cell lines. **MB-*m*-borate** has been successfully used for bioimaging in the mouse model of melanoma, further highlighting its potential diagnostic application. Overall, our work demonstrates the potential of a dual-locked fluorescent probe in the precise diagnosis of melanoma, and similar design strategies may apply in other biosystems.

https://doi.org/10.1021/acs.analchem.1c04058
Anal. Chem. XXXX, XXX, XXX−XXX

■ ASSOCIATED CONTENT

Supporting Information

The Supporting Information is available free of charge at https://pubs.acs.org/doi/10.1021/acs.analchem.1c04058.

Experimental details, synthetic procedures, optical properties of **MB-*m*-borate** and **MB-*m*-phenol**, HPLC analysis, bioimaging of **MB-*m*-borate** and **MB-*m*-phenol** in cells and mice, and compound characterization data (NMR spectra and ESI mass spectra) (PDF)

■ AUTHOR INFORMATION

Corresponding Authors

Guorui Li − *Institute of Chemical Biology and Nanomedicine (ICBN), State Key Laboratory of Chemo/Biosensing and Chemometrics, School of Biomedical Sciences, Hunan University, Changsha, Hunan 410082, China*; Email: liguorui@hnu.edu.cn

Jing Huang − *Institute of Chemical Biology and Nanomedicine (ICBN), State Key Laboratory of Chemo/Biosensing and Chemometrics, School of Biomedical Sciences, Hunan University, Changsha, Hunan 410082, China*; orcid.org/0000-0002-5494-378X; Email: huangjing16@hnu.edu.cn

Authors

Haiyue Peng − *Institute of Chemical Biology and Nanomedicine (ICBN), State Key Laboratory of Chemo/Biosensing and Chemometrics, School of Biomedical Sciences, Hunan University, Changsha, Hunan 410082, China*

Ting Wang − *Institute of Chemical Biology and Nanomedicine (ICBN), State Key Laboratory of Chemo/Biosensing and Chemometrics, School of Biomedical Sciences, Hunan University, Changsha, Hunan 410082, China*

Quan Yuan − *State Key Laboratory of Chemo/Biosensing and Chemometrics, College of Chemistry and Chemical Engineering, Hunan University, Changsha, Hunan 410082, China*; orcid.org/0000-0002-3085-431X

Complete contact information is available at: https://pubs.acs.org/10.1021/acs.analchem.1c04058

Author Contributions

H.P. and T.W. contributed equally to this work. J.H. and G.L. conceived the idea and supervised the project. G.L. and H.P. synthesized the probes. H.P. performed the in vitro assays, and T.W. carried out cell imaging experiments. H.P. and T.W. conducted the in vivo experiment. H.P. and T.W. wrote the original draft. J.H., G.L., and Q.Y reviewed and revised the manuscript. All authors approved the final manuscript.

Notes

The authors declare no competing financial interest.

■ ACKNOWLEDGMENTS

This work was funded by the National Natural Science Foundation of China (31871365 and 22177029) and the Fundamental Research Funds for the Central Universities.

■ REFERENCES

(1) Sung, H.; Ferlay, J.; Siegel, R. L.; Laversanne, M.; Soerjomataram, I.; Jemal, A.; Bray, F. *CA Cancer J. Clin.* **2021**, *71*, 209−249.

(2) Chyan, W.; Raines, R. T. *ACS Chem. Biol.* **2018**, *13*, 1810−1823.

(3) Liu, H. W.; Chen, L. L.; Xu, C. Y.; Li, Z.; Zhang, H. Y.; Zhang, X. B.; Tan, W. H. *Chem. Soc. Rev.* **2018**, *47*, 7140−7180.

(4) Li, H. D.; Kim, D.; Yao, Q. C.; Ge, H. Y.; Chung, J.; Fan, J. L.; Wang, J. Y.; Peng, X. J.; Yoon, J. *Angew. Chem. Int. Ed.* **2021**, *60*, 17268−17289.

(5) Wang, R.; Han, X.; You, J.; Yu, F.; Chen, L. *Anal. Chem.* **2018**, *90*, 4054−4061.

(6) Wang, Y.; Yu, F.; Luo, X.; Li, M.; Zhao, L.; Yu, F. *Chem. Commun.* **2020**, *56*, 4412−4415.

(7) Wu, L. L.; Huang, J. G.; Pu, K. Y.; James, T. D. *Nat. Rev. Chem.* **2021**, *5*, 406−421.

(8) Zhang, C. Y.; Zhang, Q. Z.; Zhang, K.; Li, L. Y.; Pluth, M. D.; Yi, L.; Xi, Z. *Chem. Sci.* **2019**, *10*, 1945−1952.

(9) Liu, C.; Zhang, R.; Zhang, W.; Liu, J.; Wang, Y. L.; Du, Z.; Song, B.; Xu, Z. P.; Yuan, J. *J. Am. Chem. Soc.* **2019**, *141*, 8462−8472.

(10) Teng, L.; Song, G.; Liu, Y.; Han, X.; Li, Z.; Wang, Y.; Huan, S.; Zhang, X. B.; Tan, W. *J. Am. Chem. Soc.* **2019**, *141*, 13572−13581.

(11) Kolanowski, J. L.; Liu, F.; New, E. J. *Chem. Soc. Rev.* **2018**, *47*, 195−208.

(12) Zhang, Y.; Yan, C.; Wang, C.; Guo, Z.; Liu, X.; Zhu, W. H. *Angew. Chem. Int. Ed. Engl.* **2020**, *59*, 9059−9066.

(13) Liu, Y.; Teng, L.; Xu, C.; Liu, H. W.; Xu, S.; Guo, H.; Yuan, L.; Zhang, X. B. *Chem. Sci.* **2019**, *10*, 10931−10936.

(14) Siegel, R. L.; Miller, K. D.; Jemal, A. *CA Cancer J. Clin.* **2019**, *69*, 7−34.

(15) Lai, X. L.; Wichers, H. J.; Soler-Lopez, M.; Dijkstra, B. W. *Chem. − Eur. J.* **2018**, *24*, 47−55.

(16) D'Mello, S.; Finlay, G. J.; Baguley, B. C.; Askarian-Amiri, M. E. *Int. J. Mol. Sci.* **2016**, *17*, 1144.

(17) Battistella, C.; McCallum, N. C.; Vanthournout, B.; Forman, C. J.; Ni, Q. Z.; La Clair, J. J.; Burkart, M. D.; Shawkey, M. D.; Gianneschi, N. C. *Chem. Mater.* **2020**, *32*, 9201−9210.

(18) Bai, M. H.; Huang, J.; Zheng, X. L.; Song, Z. B.; Tang, M. R.; Mao, W. X.; Yuan, L. B.; Wu, J.; Weng, X. C.; Zhou, X. A. *J. Am. Chem. Soc.* **2010**, *132*, 15321−15327.

(19) Li, G.; Yang, Y.; Zhang, Y.; Huang, P.; Huang, J. *CCS Chem.* **2021**, *3*, 1−40.

(20) Peng, M.; Wang, Y.; Fu, Q.; Sun, F.; Na, N.; Ouyang, J. *Anal. Chem.* **2018**, *90*, 6206−6213.

(21) Zhang, J.; Li, Z.; Tian, X.; Ding, N. *Chem. Commun.* **2019**, *55*, 9463−9466.

(22) Wu, X. F.; Li, L. H.; Shi, W.; Gong, Q. Y.; Ma, H. M. *Angew. Chem., Int. Ed.* **2016**, *55*, 14728−14732.

(23) Wu, X. F.; Li, X. H.; Li, H. Y.; Shi, W.; Ma, H. M. *Chem. Commun.* **2017**, *53*, 2443−2446.

(24) Li, Z.; Wang, Y. F.; Zeng, C.; Hu, L.; Liang, X. J. *Anal. Chem.* **2018**, *90*, 3666−3669.

(25) Szatrowski, T. P.; Nathan, C. F. *Cancer Res.* **1991**, *51*, 794−798.

(26) Chang, M. C. Y.; Pralle, A.; Isacoff, E. Y.; Chang, C. J. *J. Am. Chem. Soc.* **2004**, *126*, 15392−15393.

(27) Miller, E. W.; Albers, A. E.; Pralle, A.; Isacoff, E. Y.; Chang, C. J. *J. Am. Chem. Soc.* **2005**, *127*, 16652−16659.

(28) Dickinson, B. C.; Chang, C. J. *J. Am. Chem. Soc.* **2008**, *130*, 9638−9639.

(29) Yuan, L.; Lin, W. Y.; Xie, Y. N.; Chen, B.; Zhu, S. S. *J. Am. Chem. Soc.* **2012**, *134*, 1305−1315.

(30) Abo, M.; Urano, Y.; Hanaoka, K.; Terai, T.; Komatsu, T.; Nagano, T. *J. Am. Chem. Soc.* **2011**, *133*, 10629−10637.

(31) Xie, X. L.; Yang, X. E.; Wu, T. H.; Li, Y.; Li, M. M.; Tan, Q.; Wang, X.; Tang, B. *Anal. Chem.* **2016**, *88*, 8019−8025.

(32) Ye, S.; Hu, J. J.; Yang, D. *Angew. Chem. Int. Ed. Engl.* **2018**, *57*, 10173−10177.

(33) Morgan, B.; van Laer, K.; Owusu, T. N.; Ezeriņa, D.; Pastor-Flores, D.; Amponsah, P. S.; Tursch, A.; Dick, T. P. *Nat. Chem. Biol.* **2016**, *12*, 437−443.

(34) Ye, S.; Hananya, N.; Green, O.; Chen, H.; Zhao, A. Q.; Shen, J.; Shabat, D.; Yang, D. *Angew. Chem. Int. Ed. Engl.* **2020**, *59*, 14326−14330.

(35) Song, X.; Bai, S.; He, N.; Wang, R.; Xing, Y.; Lv, C.; Yu, F. *ACS Sens.* **2021**, *6*, 1228−1239.

(36) Zhang, C.; Jiang, D.; Huang, B.; Wang, C.; Zhao, L.; Xie, X.; Zhang, Z.; Wang, K.; Tian, J.; Luo, Y. *Technol. Cancer Res. Treat.* **2019**, *18*, No. 1533033819894331.
(37) Ji, Y.; Dai, F.; Yan, S.; Shi, J. Y.; Zhou, B. *J. Agric. Food Chem.* **2019**, *67*, 9060−9069.
(38) Solomon, E. I.; Heppner, D. E.; Johnston, E. M.; Ginsbach, J. W.; Cirera, J.; Qayyum, M.; Kieber-Emmons, M. T.; Kjaergaard, C. H.; Hadt, R. G.; Tian, L. *Chem. Rev.* **2014**, *114*, 3659−3853.

https://doi.org/10.1021/acs.analchem.1c04058
Anal. Chem. XXXX, XXX, XXX−XXX